Forest and Society
Vol. 7(1): 150-168, April 2023
doi: 10.24259/fs.v7i1.24526

REGULAR RESEARCH ARTICLE

Urban Green Space Analysis and its Effect on the Surface Urban Heat Island Phenomenon in Denpasar City, Bali

I Kade Alfian Kusuma Wirayuda [1,*], Prima Widayani [2], Andung Bayu Sekaranom [2]

AFFILIATIONS

1. Graduate School, Universitas Gadjah Mada, Yogyakarta, Indonesia
2. Faculty of Geography, Universitas Gadjah Mada, Yogyakarta, Indonesia

*Corresponding author:
kadealfian98@mail.ugm.ac.id

ABSTRACT

The Urbanization process in Indonesia's big cities causes adverse environmental impacts such as climate change and land cover change. Urban climate change causes the warming of urban areas compared to rural areas; it is called Urban Heat Island phenomenon. Loss of vegetation due to urban development is one of several causes that contribute to urban heat islands. This study examines the availability of green spaces and their effects on the surface urban heat island in Denpasar city. This study used the spatial approach for Urban Green space mapping with digitizing methods. Landsat 8's thermal band is used for land surface temperature mapping and to conduct a spatial pattern analysis of the SUHI phenomena. The Global Moran's Index and Local Indicator of Spatial Association (LISA) were used to determine the correlation between urban green space and SUHI. The study result shows that Denpasar City's urban green space area covers 28.22 km2. That's equal to 22.1% of the Denpasar City Administrative area. Denpasar Selatan district has the largest urban green space cover, with 14.19 km2 covered, or 50.27% of all the green space in Denpasar City. The majority of Denpasar is affected by UHI occurrences, except the northern region of North Denpasar and the southern region of South Denpasar. The maximum UHI level reaches 4-5°C, located on the east side of South Denpasar, especially in the Sanur coastal area. According to the spatial pattern study, the association between urban green space and SUHI only exists on the north side of Denpasar. The correlation between low-SUHI intensity clusters and high cover of green space is shown in the same area. However, the association between High-UHI intensity and low green space cover has not significantly happened. It indicated that other factors besides green space could affect the land surface temperature.

KEYWORDS

Urban green spaces; Urban heat island; Remote sensing; Spatial analysis; Spatial autocorrelation;

RECEIVED 2022-12-14
ACCEPTED 2023-03-25

1. INTRODUCTION

Over the past thirty years, Indonesia's major cities have seen significant growth in the urbanization process (Setiawan et al., 2006). This process has detrimental effects on the environment, such as land cover change and pollution, which can affect the physical, biological, and chemical elements in an ecosystem and also contribute to climate change (Grimm et al., 2008). Urban climate change causes phenomena such as urban temperature warming and affects warmer urban areas relative to rural areas. This phenomenon is called "Urban Heat Island" (UHI) (Karl et al., 1988; Lo & Quattrochi, 2003). The urban area's warming is caused by anthropogenic activity such as transportation, power plants, and other heat sources (Memon et al., 2008).

Another factor causing UHI is the shift in land cover from natural to built-up areas (Yamamoto, 2006). Vegetation cover is a radiation absorbent. The loss of vegetation has an impact on this process, and the radiation absorbs by built-up cover with high heat capacity. Raise of urban air temperature affect thermal comfort (Akbari et al., 2001;

Quattrochi et al., 2000). The UHI phenomenon is divided into two types: i.e., atmospheric urban heat islands and surface urban heat islands (SUHI). The Atmospheric UHI occurs in the atmosphere, and it is characterized by higher air temperatures in urban areas compared to rural areas. Atmospheric UHI has two types: canopy layer UHI (CLUHI) and boundary layer UHI (CLUHI). CLUHI occurs on the air temperature of the canopy layer (above the surface until under the top of a tree or building), which is the human activity area. In the contrary, the BLUHI occurs above the canopy layer until the area where the urban landscape does not affect the atmosphere (under 1.5 km above the ground) (United States Environmental Protection Agency, 2008). The surface UHI (SUHI) occurs at the Earth's surface and is specified by the temperature difference. Therefore, the detection of surface urban heat islands is identified through the land surface temperature with a remote sensing approach (Li et al., 2011; Voogt & Oke, 2003). Vegetation has an important impact on UHI because it reduces surface and air temperatures through the evapotranspiration process. Other factors that can affect UHI such as urban material properties with a high heat capacity, urban geometry, anthropogenic heat sources, and other factors such as weather and geography

Denpasar is one of Indonesia's cities that has a high population, with the 23rd high population rank of 98 cities in Indonesia, with an area of 127.78 km2. City development affects land use changes and reduces the availability of green space. The loss of green space will have an impact on the UHI phenomenon. Denpasar's SUHI study has previously done (As-Syakur et al., 2012) to detect the SUHI phenomenon in 1995–2003. The study result shows the temperature pattern with high temperatures clustered in the downtown area and reduced toward the rural area. Urban green space is an important factor in reducing the UHI effect. It also has a biodiversity conservation function, an aesthetic function, and a social-education function. According to Indonesia's Republic Law of Spatial Planning, green space in an urban area must encompass 30% of the city area. 20% of it is allocated to public green space and the other 10% is shared with private green space. This study examines the availability of green spaces and their effects on the surface urban heat island (SUHI) and several other parameters, such as surface humidity and building density.

2. MATERIALS AND METHODS

2.1 Study area

This research was conducted in the city of Denpasar, with an area of 127.78 km2. Located between 08 35' 31" - 08 44' 49" South Latitude and 115 10' 23"–115 16' 27" East Longitude, Denpasar consists of four sub-districts i.e., Denpasar Barat (West Denpasar), Denpasar Utara (North Denpasar), Denpasar Timur (East Denpasar), and Denpasar Selatan (South Denpasar) (Figure 1). Population census data shows that Denpasar's population is around 725,314 people.

2.2 Data

Field measurement data and remote sensing data were used in this study. The remote sensing data used is obtained from remote sensing data service providers. The remote sensing data used is shown in Table 1.

Table 1. Remote sensing data used for the study

No	Data	Purpose	Source
1.	World Imagery maps (2022)	Urban green space mapping	*ESRI*
2.	Landsat 8 Image (September 9, 2022)	SUHI analysis	USGS Science

No	Data	Purpose	Source
3.	Denpasar's administrative shapefile	Study border	Geospatial information agency of Indonesia

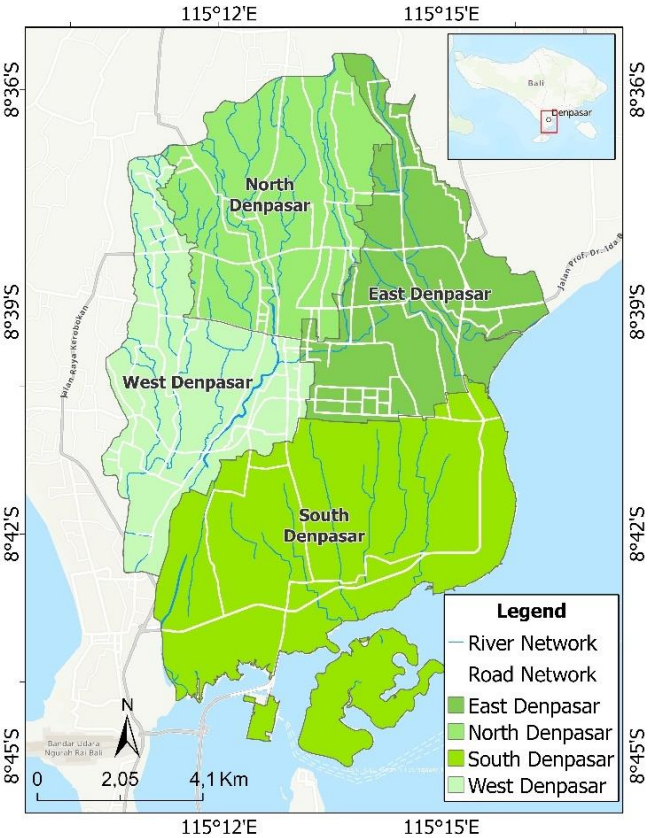

Figure 1. Study site

2.3 Method

2.3.1 Urban green space mapping

The urban green space map was obtained by interpreting the World Imagery data with the "on-screen digitizing" method to create a vector map. This method was selected to simplify the identification process of urban green space types. The green space typologies are according to Indonesia's Ministry of Public Works and Housing regulation of Green Space provision in urban areas. In general, the green space type is differentiated into Private and Public green space. The Private green space consists of Courtyard (home yard, office yard, & business yard). However, Public green space consists of Cities parks & forests, road green lines, and Specific Function green space (river border, beach border, & cemetery green space). Rice fields were excluded from the green space category in this study. According to some recent studies, the rice field has an impact on climate change. During certain seasons, rice fields can emit greenhouse gases such as methane (CH4) and nitrogen dioxide (N2O). Methane gas was produced during the organic decomposition process by anaerobic bacteria while the rice field was flooded (Johnson et al., 2007; Sass & Cicerone, 2002).

To determine the validity of the interpretation results, a field verification process was carried out based on the green space vector map. Verifications were carried out at 150 sites, which were divided into three categories: public green space, private green space, and non-green space (50 locations for each class). An error matrix or confusion matrix was created from the field verification data. With Kappa Accuracy, the confusion matrix was used to calculate the accuracy level. For high accuracy, Kappa scores of at least 85% are required (Lillesand et al., 2015).

2.3.2 Surface urban heat island mapping

The analysis of surface urban heat islands was based on land surface temperature patterns. The Thermal Band (band 10) of the Landsat 8 image was used for land surface temperature mapping. The processing steps for land surface temperature are as follows:

- Land surface temperature estimation
  ToA radiance correction aimed to minimize the radiometric distortion of the image caused by the sun's position on the object and convert the digital number value to radiance value (USGS, 2013). The following equation is used in the correction process. The correction process uses the following equation:

  $$L\lambda = MLQcal + AL \quad (1)$$

  Lλ is ToA Spectral Radiance, and ML is Radiance multiplicative band, AL is Radiance add band, and Qcal: Pixel value

- Brightness of Temperature Calculation
  The brightness of temperature is calculated by converting the ToA spectral radiance value with the equation 6 (USGS, 2013)

  $$BT = \frac{K2}{ln\left(\frac{K1}{L\lambda}+1\right)} \quad (2)$$

  BT is the Brightness Temperature (Kelvin) and subtracted 275.15 to convert to celcius, Lλ: TOA spectral radiance, K1: K1 Calibration Constant Band, K2: K2 Calibration Constant Band

- Vegetation index calculation
  Normalized Difference Vegetation (NDVI) calculation was done using the Near Infra-red (band 5) and red band (band 4) of Landsat 8 (Rouse et al., 1977) with the following equation:

  $$NDVI = \frac{NIR-RED}{NIR+RED} \quad (3)$$

  NDVI is the vegetation index; NIR is Near Infra-red band; Red is the red band

- The proportion of vegetation (Pv) calculation
  The NDVI value was used to calculate the proportion of vegetation. The PV calculation uses equation 8 (Carlson & Ripley, 1997).

  $$Pv = \left(\frac{NDVI-NDVImin}{NDVImax-NDVImin}\right)^2 \quad (4)$$

  Pv= Vegetation proportions, NDVI= NDVI value, NDVImax= Highest NDVI value (vegetation), NDVImin= lowest NDVI value (soil).

- Emissivity value calculation
  The Pv value was used to calculate the emissivity value with the following equation

$$\varepsilon = VePv + Se\ (1 - Pv) + 4 < de > \ 0.06Pv(1 - Pv) \quad (5)$$

$$\varepsilon = 0.985Pv + 0.960\ (1 - Pv) + 0.06\ Pv(1 - Pv)$$

*e is the emissivity; Ve is vegetation emissivity (0.985), and Pv is the proportion of vegetation, Se is soil emissivity (0.960), 4*de= 0.06 (constant average)*

- Land surface temperature
  The Land surface temperature was calculated with equation 6 (Stathopoulou & Cartalis, 2007).

$$T_S = \frac{BT}{\left(1+\frac{\lambda BT}{\partial}\ln \varepsilon\right)} \quad (6)$$

T_S is the surface temperature; BT is the Brightness temperature; λ is the radiance wavelength; ∂ is Constant 1.438 x 10^{-2}mK, and e is the Emissivity value

2.3.3 Surface Urban heat island identification

The surface temperature threshold was used to identify SUHI (Ma et al., 2010). The UHI value is calculated with the following equation:

$$UHI = T_s - (\mu + 0{,}5\ \alpha) \quad (7)$$

UHI is the Urban Heat Island; T_s is the surface temperature; μ is the surface temperature mean; α is the surface temperature standard deviation. An area is identified as UHI if the threshold value is T>0; however, if the value is 0<T indicates the non-UHI area

2.3.4 Surface moisturize index

Humidity is related to land surface temperature. It has a negative correlation, showing an inverse relationship. Low humidity usually indicates a high temperature. Surface humidity can be calculated with the Normalized Difference Moisture Index (NDMI), which uses the Shortwave Infrared/SWIR (band 6) wavelengths (band 5). It uses the following equation to calculate:

$$NDMI = \frac{NIR-SWIR}{NIR+SWIR} \quad (8)$$

2.3.5 Built-up density index

Built-up density is one of the factors that can affect the UHI phenomenon. The normalized difference built-up index (NDBI) is one method that can be used to analyze the built-up density. NDBI calculations use the Near Infrared (NIR) and Shortwave Infrared (SWIR) (Zha et al., 2003) bands. The built-up Index was calculated using the equation below.:

$$NDBI = \frac{SWIR-NIR}{SWIR+NIR} \quad (9)$$

2.3.6 In-situ measurement

In-situ measurement was aimed to obtain the surface temperature and air temperature from the field data. The in-situ surface temperature data will be compared to the satellite image land surface temperature value to determine the value difference. LST data were collected at 15 observation points throughout the study area (Figure 2b). The sampling points were determined using the purposive sampling method on three different land covers, i.e., the built-up area, the bush and rice field, and the vegetation area. The data were collected on September 9, 2022, at the same time as the image acquisition times. Landsat 8 is a sun-synchronous satellite, acquiring images every 16

days at +/- 15 minutes at 10:00 am local time. Therefore, the data measurement process is carried out in the time range of 9 to 10 am. The air temperature measurements are means to compare differences in air temperature in the green space and its surroundings. The pattern of air temperature during the daytime and nighttime will be obtained.

The air temperature was measured in five different locations. One point is located in the public green space, and four others are in the surrounding area (Figure 2a), specifically in the built-up area. The points around green spaces have varying levels of building and vegetation density, from low to moderate. The temperature data was collected using a temperature logger. The determination of air and surface temperature sampling locations is also based on the building density index map and vegetation density. The field sampling location map is shown in Figure 1.

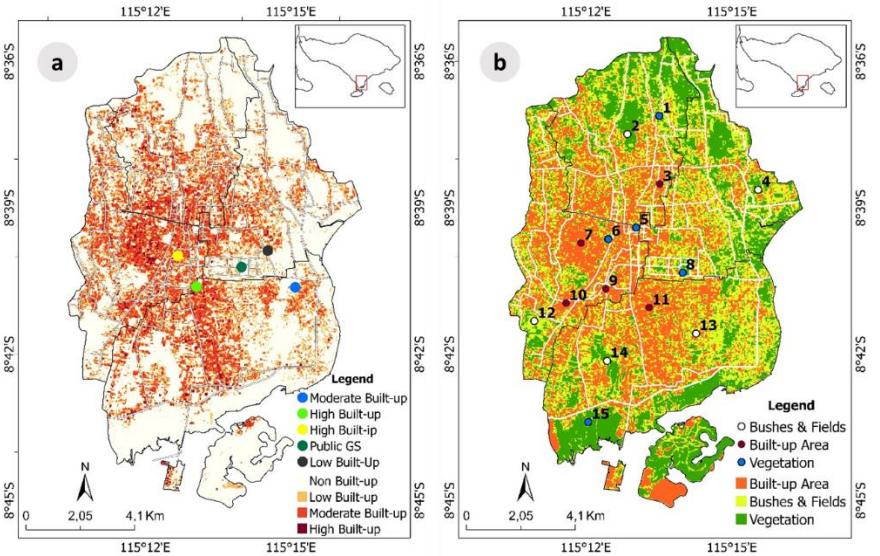

Figure 1. (a) Air temperature sampling sites and Built-up density maps (b) Surface temperature sampling sites and vegetation cover maps.

2.3.7 Correlation analysis

The correlation analysis was used to find out the relationship between green space and the phenomenon of surface urban heat islands. The sample quantity was determined using the systematic sampling method. The sample was determined by dividing the study area into several grids. Every grid will cover the average LST value, NDMI value, and green space cover. Each grid was 500 x 500 m in size. Grid systems are used to simplify the autocorrelation analysis process and produce a proportional number of grids in the study area. The grid value contained the average pixels value within that grid. The total grid sample in the entire study area is 451, thus, the correlation analysis is based on 451 grid data.

The spatial-based correlation analysis was applied for the correlation analysis, considering the study was spatial-based. Spatial autocorrelation is a spatial-based analysis that can be used to determine the correlations between the values of a variable. Autocorrelation analysis is used to determine the relationship between observed values on the same variable (self-correlation) (Anselin, 1994; Griffith, 2005). The results of the analysis can be positive, negative, or uncorrelated. A positive correlation indicates that the value is similar at the nearby site (clustered value). A

negative correlation indicates that the value in the neighboring location is different (spread value). The uncorrelated result displays a random pattern value (Lee & Wong, 2001). One of the spatial autocorrelation analyses is Moran's Index (Gittleman & Kot, 1990). Moran's index value ranged between -1 and 1. A negative correlation is shown by the index value of $-1 < I \leq 0$. Unlike $0 < I \leq 1$, which implies a positive correlation. Moran's Index was a global examination that wasn't able to demonstrate a correlation in specific areas. As a result, an extension approach is required to assess the correlation in a specific area. A local analysis can be performed using the Local Indicator of Spatial Association (LISA). The spatial pattern can be known from the Z-score. A Z-score between 1.65 to >2.58 has a Clustered pattern, -1.65 until 1.65 will be a random pattern, and under -1.65 generate a dispersed pattern.

The purpose of LISA analysis was to find out the autocorrelation coefficient in a specific area. This analysis yields a signification map, cluster maps, and Moran's scatter plot. The signification maps show the influence level of a data value on other values. The cluster maps show an area that has a clustered pattern of data. Whereas, the Moran scatter plot shows the data spread in four quadrants. The first quadrant is called High-High (HH), which describes an area with a high value and is surrounded by a high value. The second quadrant is Low-High (LH), representing a low data value that is surrounded by a high value. The third quadrant called the Low-Low quadrant (LL) describes a low data value surrounded by low data value too. And the Fourth quadrant is High-Low (HL), representing a high data value surrounded by a low data value.

3. RESULTS

3.1 Urban Green Space Analysis

The analysis results show that the distribution of urban green space is distributed throughout Denpasar. The highest density of green space is on the south side of Denpasar, which is Ngurah Rai Mangrove Forest. The urban green space covers 28.22 km2, or 22.1% of the 127.78 km2 Denpasar City area, with 14.12 km2 (11.05%) being public green space and 14,10 km2 (11.03%) being private green space (Figure 3a). Green space in an urban area must cover 30% of the city area, according to Indonesian Law on Spatial Planning. It is divided into 20% for public green space and 10% for private green space. Accordingly, the green space availability has not occupied the minimum criteria, with the 11.44 km2 deficit of public green space. Denpasar's green space type is dominated by a private green space (yard), followed by a specific function of green space, such as a river and beach border with 8,08 km2. The city park has a total area of 4.91 km2, and the road green line type has the smallest cover (1.12 km2) (Figure 3 & Table 2). Denpasar Selatan has the highest green space cover, with 14.19 km2 or 50% of Denpasar's green space cover. This is due to the existence of the Ngurah Rai Mangrove Forest in this subdistrict. Denpasar Barat has the least amount of green space, with 3.55 km2 (or 12,58% coverage) (Table 2).

Table 2. Green space distribution area

Study Area	Yard	City Park	Road Green Line	Specific Function	Total (km^2)	(%)
Denpasar Barat	2.77	0.25	0.15	0.37	**3.55**	12.58
Denpasar Utara	2.79	0.71	0.19	1.20	**4.89**	17.33
Denpasar Timur	2.95	1.09	0.49	1.06	**5.59**	19.82
Denpasar Selatan	5.58	2.87	0.29	5.45	**14.19**	50.27
Total	**14.10**	**4.91**	**1.12**	**8.08**	**28.22**	**100**

South Denpasar has the most yard green space, with 5.58 km2. The residential yard dominates with an area of 4.05 km2, which is more significant than other sub-districts. The largest availability of open land in South Denpasar may influence residential Yard provision. In other areas with limited land availability, the provision of green space in the house's yard is limited. The Business Yard in South Denpasar is also the largest area from other areas with 1.28 km2. This is due to South Denpasar being one of the tourism industry areas, so there are many supporting accommodations such as hotels and villas, which are required to provide green space. However, the highest Office Yard green space grounds are in East Denpasar with an area of 0.31 km 2 which is an office center area.

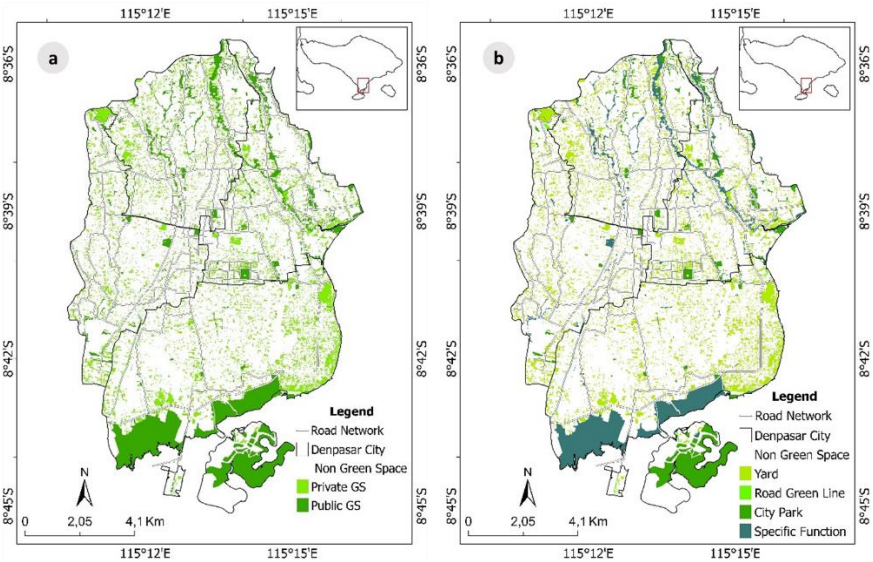

Figure 3. (a) Public and private green spaces maps (b) Green space type maps

The verification of urban green space at 150 locations shows six misinterpretations of the green space map, shown in Conffusion matrix table (Table 3). The error was spotted in the private green space class. It is caused by a shift in land cover from vegetation to built-up areas. The interpretation accuracy is 94%, according to the Kappa Accuracy calculation. Lillesand and Kiefer (1979) defined an accurate interpretation as having a Kappa accuracy greater than 85%.

Table 3. Conffusion matrix table

Classification data	Reference data			Total	User Accuracy
	Public GS	Private GS	Non GS		
Public GS	50	0	0	50	100%
Private GS	0	44	6	50	88%
Non GS	0	0	50	50	100%
Total	50	44	56	150	
Producer Accuracy	**100%**	**100%**	**89,29%**		
Overall accuracy			**96%**		
Kappa accuracy			**94%**		

3.2 Surface Urban Heat Island Analysis

The LST map is used to identify Surface Urban Heat Islands at Denpasar City. The Landsat 8 imagery used to produce the LST maps was acquired in August and September. It is related to the LST validation process from field checking, which was

carried out concurrently during the image acquisition process. The Landsat image used for analysis is the clearest from cloud cover. From four image acquisitions in August until September 2022 period, the clearest image was acquired on 9 September. The LST map shows that the surface temperature in Denpasar city on September 9 ranged from 15 to 26 °C (Figure 6a). The LST pattern reveals a significant difference in which side of the city is cooler on the north and south sides. The lowest temperature is on the city's northern side, which is a rice field area. A flooded rice field area will affect the surface temperature value recorded on the image. The highest temperature is around 26 °C, which is found on the east side of Denpasar.

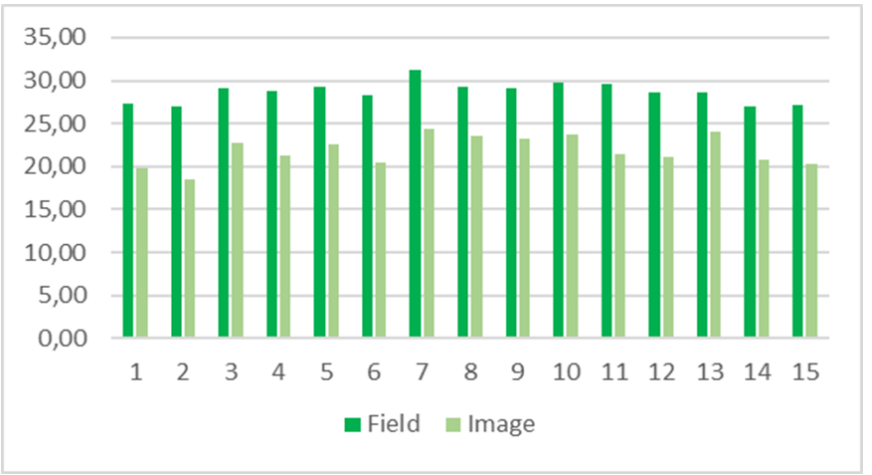

Figure 4. Surface temperature graph comparing image processing results to field measurements

This LST map shows a different pattern from previous research by Asmiwyati et al. (2020), which used a Landsat image on March 19th, 2018. The differences lie in the temperature pattern and range. That study shows a higher temperature range, which is 23 to 31°C, and the temperature pattern shows the highest temperature is in the city center. In the contrary, the LST map on September 9 shows the highest temperature was located on the east side. The result difference may be caused by the difference in image acquisition time. Asmiwyati (2020) used a Landsat image that was acquired during a dry season (March), and this study used a wet season image (September). The four-year gap in the study may also affect the land cover and anthropogenic activity in Denpasar City. The surface temperature is inversely related to the surface humidity. The area with a high surface temperature has a low moisture index value (Figure 6b). On the other hand, low-temperature locations have a high moisture index value. High surface humidity is in north and south Denpasar. It is caused by the existence of mangrove forest areas in southern Denpasar and northern Denpasar rice fields which are inundated by water. However, West Denpasar and East Denpasar show relatively lower surface moisture indexes. This is due to the low vegetation cover in the area. Surface humidity is also affected by building density. Areas with high surface humidity in North and South Denpasar are non-built-up areas (Figure 2a). The high built-up density is in West Denpasar, the north side of South Denpasar, and the south side of North Denpasar, which shows a low surface humidity. Surface humidity can affect the surface emissivity. The surface emissivity of an object indicates its ability to emit energy. A high-emissivity object can absorb and radiate more energy than a low-emissivity one (Sabin, 2007 in Fawzi, 2014). Vegetation and water cover have high emissivity values. According to

Utomo et al. (2017), emissivity influences surface temperature but is also impacted by other parameters, such as an object's thermal conductivity and thermal capacity. The surface temperature tends to be lower if an object has low thermal conductivity, even if it has a high emissivity and thermal capacity value (Utomo et al., 2017).

The estimated land surface temperature from image processing was compared to the measured land surface temperature from field inspection. The comparison chart reveals a large temperature difference (Figure 4). The temperature difference between the two readings at site 15 of the field temperature sampling exceeds 8.5 °C. Temperature discrepancies can be produced by differing measuring scales. A temperature measurement with an infrared pyrometer only covers a narrow area. On the other hand, the satellite image can cover a 100x100-meter area in a single pixel. Moreover, the measurement distance from the surface and sensor capabilities can influence the temperature value. The Pearson correlation study reveals a substantial association between the image's temperature value and the field temperature. The Pearson correlation coefficient is 0.88 (close to 1). It shows it has a similar temperature value pattern to those two. Therefore, even though there is a reasonably high difference in value, the pattern of temperature values at the point of observation can be said to be similar.

Air temperature measurements have been conducted in five locations for two weeks. The air temperature chart shows the air temperature's mean trendline. The chart fluctuation (Figure 5) shows a similar pattern at all location points, with the highest temperature occurring at 1 pm. The temperature difference does not seem significant between location points except in the commercial area with high built-up density. The air temperature difference seems significant starting at 9 a.m., which can be affected by sun irradiation. The air temperature difference between the Urban Green Space and other locations does not seem very significant, even though it is higher than the two other locations. It may be due to the green space being surrounded by roads and the office center area. It causes the area to be heavily trafficked, and anthropogenic activities can be a factor in increasing the air temperature. If the air temperature is compared to the surface temperature from Landsat image processing, the air temperature seems higher than the surface temperature at 10 pm (image acquisition time).

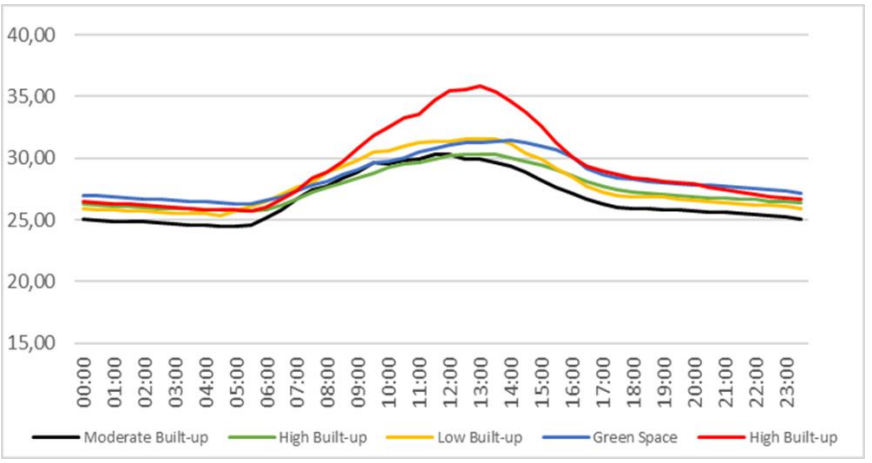

Figure 5. Air temperature observation chart

To conduct a SUHI analysis, the study area was broadened to determine the differences between urban and rural conditions (Figure 6c). The expansion took place

in the district administrative region surrounding Denpasar City, specifically in the Badung and Gianyar Districts. Based on the SUHI maps, the SUHI phenomena occurred in Denpasar and several regions in the adjacent districts. A significant SUHI phenomenon was seen outside of Denpasar City in the Badung district (west of Denpasar), especially in locations with SUHI >5°C classes, which is a Ngurah Rai Airport area. Whereas, the SUHI phenomena in the Denpasar city (Figure 6d) area show a similar pattern with the land surface temperature.

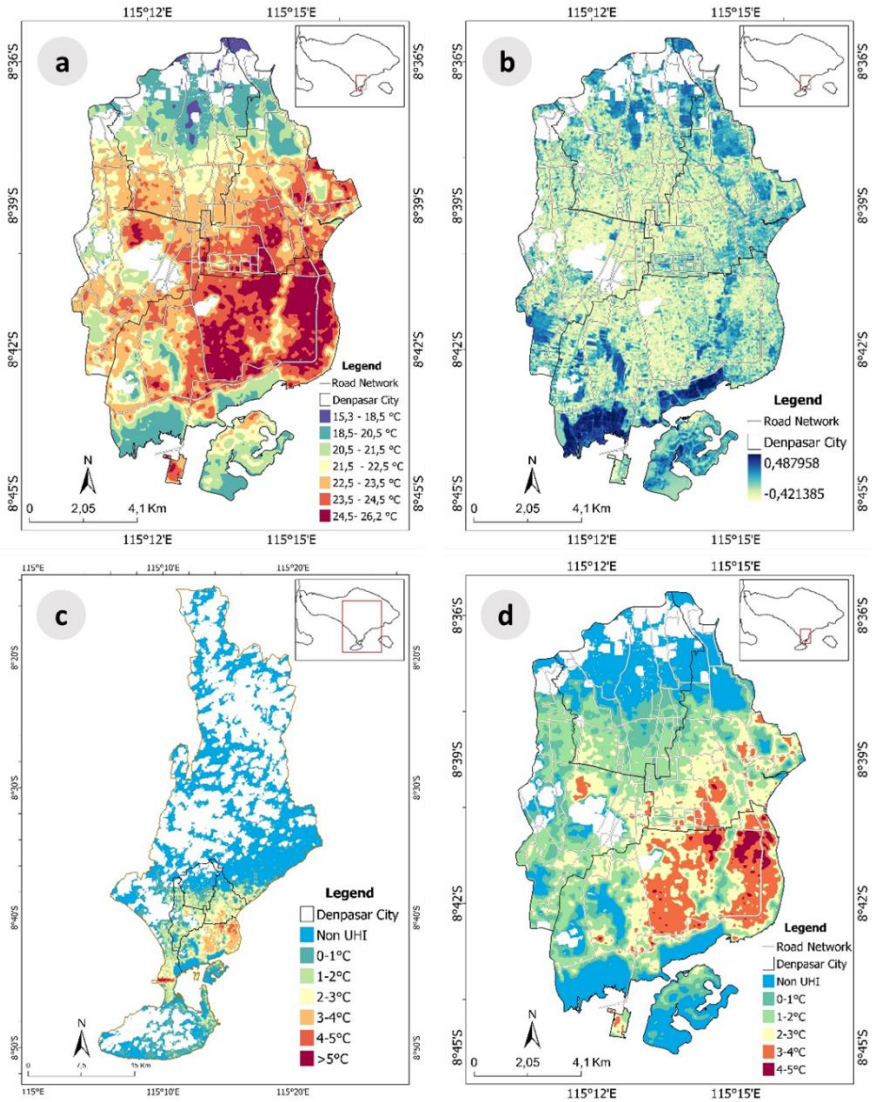

Figure 6. (a) Land surface Temperature maps (b) Land surface moisture index maps (c) Surface Urban Heat Island around Denpasar (d) Surface Urban Heat Island in Denpasar City

The SUHI phenomenon occurs in almost all areas of Denpasar City, except on the north side in the North Denpasar and on the south side in South Denpasar, which are rice fields and mangrove areas. The highest SUHI class in the Denpasar area was 4-5 °C

that located in east part of South Denpasar, which was also the highest surface temperature. The area with the highest temperature has a low-to-high building density and sparse to moderate green space cover. According to the United States Environmental Protection Agency (2008), the other factor that can affect the UHI phenomenon besides the vegetation cover is, among others, urban material properties, urban geometry, anthropogenic activity, and other factors such as geographic conditions and weather. Therefore, that factor can affect the land surface temperature in this area. The high-SUHI area in the east part of South Denpasar is the Sanur coast area, which is a tourism destination area. This area has many accommodation buildings for tourism support and quite high anthropogenic activity. Moreover, this area is a lowland that generally has a higher temperature than a highland.

South Denpasar has the largest SUHI phenomenon, covering 36.89 km2. However, East Denpasar has the highest percentage of SUHI, with 75.80% of the sub-district area (Table 4). North Denpasar has the lowest SUHI phenomenon, which only covers 10.6 km2 or 40% of the North Denpasar sub-district area. South Denpasar has the widest green space, but it is also the most affected by the SUHI phenomenon. It can happen as a result of the uneven distribution of green spaces. South Denpasar's green space is concentrated in the southern region, which is in the Mangrove Forest area, with a high density of vegetation. South Denpasar also has the highest green space with 5.58 km2 but has the highest SUHI intensity value. SUHI is a phenomenon that is influenced by many factors. In addition to land cover and anthropogenic activity, SUHI can also be affected by weather and surface conditions. The remote sensing approach for the identification of SUHI is strongly influenced by atmospheric and surface conditions, which can affect the values recorded in the image. According to the UHI level map, the UHI phenomena have affected the majority of the Denpasar city region, which is characterized by higher temperatures in the downtown area compared to the surrounding areas.

Table 4. SUHI Phenomenon Distribution

Study Area	SUHI Area (km2)	%
East Denpasar	20,57	79,42
South Denpasar	36,89	75,80
West Denpasar	17,19	71,00
North Denpasar	10,60	40,12

3.3 Correlation test

The correlation test aims to determine the relationship between SUHI, urban green space, surface moisture, and built-up density. Spatial autocorrelation determines a variable's spatial pattern and the relationship between data values.

3.3.1 Urban Green Space autocorrelation test

Moran's Index value of the green space variable is 0.59, which means a positive autocorrelation occurred in this variable. A positive autocorrelation indicates that the adjacent green space tends to have similar areas. The P-value above 0.05 (0,88) means there is a significant influence of a value on other values. The urban green space variable shows a clustered spatial pattern described by a 24.14 z-score value. The local indicator (LISA) analysis results in the form of a signification map (Figure 9), cluster map (Figure 10), and Moran's scatter plot (Figure 8). The significant maps show the signification level of the relationship between locations. The signification level of the green space variable shows an insignificant relationship between the surrounding area. Moran's scatter plot shows the point spread on the 1st quadrant (High-High), 2nd

quadrant (Low-High) 3rd quadrant (Low-Low), and 4th quadrant (High-Low). The LH quadrant means the low-cover areas of green space are surrounded by a high-cover area of green space. On the other hand, the HL quadrant shows a high area of green space surrounded by a low cover of green spaces. The LL quadrant indicates a low area of green space also surrounded by low-cover areas. The green space's cluster map shows the distribution of cluster patterns. The cluster pattern is dominated by LL and LH quadrant areas which are scattered in groups.

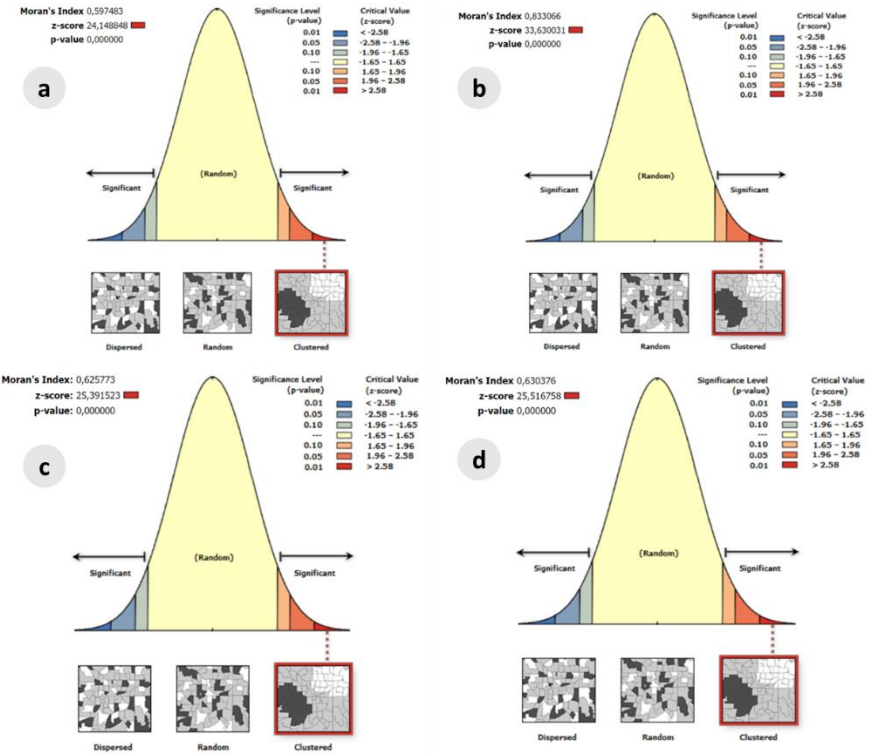

Figure 7. Global Moran's Index result of (a) Green space (b) Land surface temperature (c) Surface moisture (d) Built-up density

3.3.2 SUHI autocorrelation test

The SUHI variable has a Moran's index of 0.83, which indicates a positive autocorrelation on this variable. A positive autocorrelation means the neighboring area has a similar value. The P-value result of 0.00 shows a significant influence of SUHI values at the adjoining locations. Based on the Z-score of 33.63 (>2.58), the spatial pattern of this variable is clustered. The significance map depicts the significant relationship between Denpasar's north and east sides. Moran's scatter plot (Figure 8b) shows the points' distribution is around the centerline, which indicates a low standard deviation of the data. The points are evenly distributed across all quadrants, with the first (High-High) and third (Low-Low) quadrants dominating. It is similar to the cluster map, which has a LL cluster on the north side and an HH on the east side of the city.

3.3.3 Surface Moisture Correlation Test

Moran's index for the moisture variable is 0.62, which indicates a positive autocorrelation on this variable. It means the neighboring surface moisture has a similar value. The influence of one value over another seems significant, as described

by the P-value of 0.00. The spatial pattern of this variable is clustered with a Z-score of 25.39. The signification map shows that the city center, north side, and south side have high significance levels. The scatter plot of this variable (Figure 8c) shows the point is spread across all quadrants but dominated by the first (High-High) and third quadrants (Low-Low). The HH quadrant means the high moisture value is surrounded by a high moisture value, and the LL quadrant means the low moisture value is surrounded by a low moisture value. Based on the cluster map, the HH cluster is located on the north and south sides of the city, whereas the LL cluster is at the city center.

3.3.4 Built-up density correlation test

The built-up density variable has a positive autocorrelation represented by Moran's index value of 0.63. It explained the neighboring location has a similar value of the built-up density. The spatial pattern forms a cluster shown by the Z-score of 25.51. Moreover, the P-value of 0.00 shows a significant influence between values, especially in the downtown area and the south side of the city. The point on the scatter plot (Figure 8d) spread at all quadrants and dominated at the HH and LL quadrants. The HH cluster is located in the downtown area, while the LL cluster at the north and south side of the city.

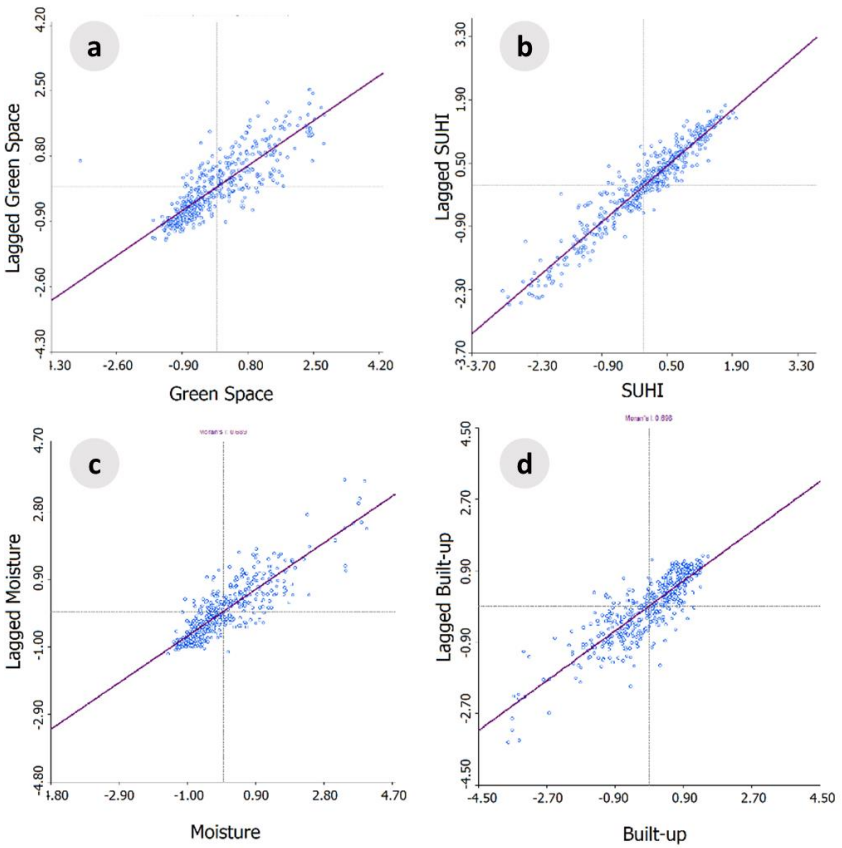

Figure 8. (a) Green space scatter plot (b) Temperature scatter plot (c) Surface moisture scatter plot (d) Built-up index scatter plot

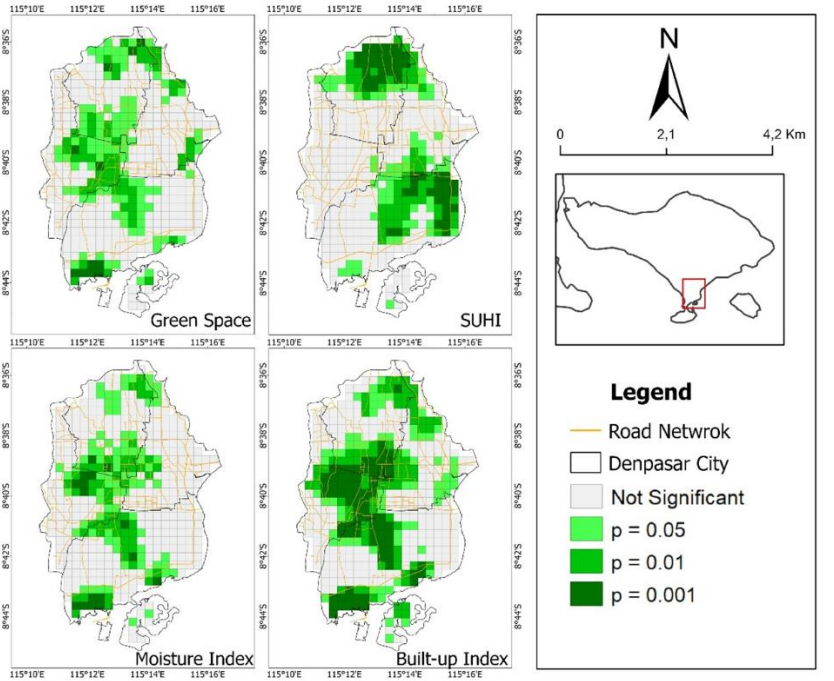

Figure 9. Sigification maps

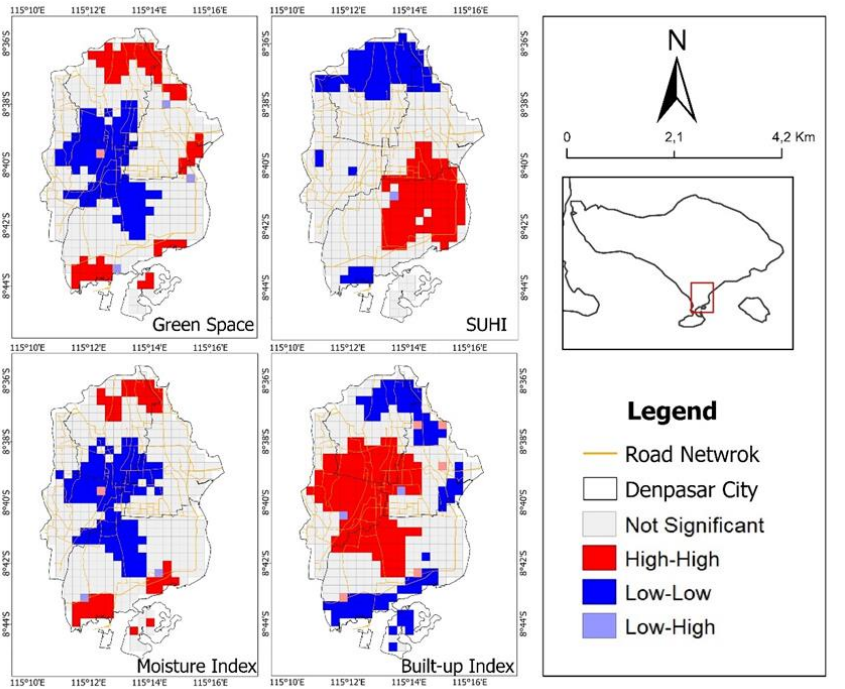

Figure 10. Cluster maps

3.4 The relation between urban green space and surface urban heat island

The relation between green space and SUHI can be known by comparing the Global Moran's and LISA analysis results. The Global Moran's index analysis shows a clustered pattern of green space and SUHI. The surface moisture and built-up density have the same spatial cluster as the SUHI. Based on the LISA analysis, the cluster map of the green space and SUHI showed various distribution patterns. It indicates the availability of green space is not the only factor that can affect the SUHI phenomenon.

The relationship between green space and SUHI occurs in a certain area. It identified at the HH cluster on the green space cluster map with the LL and LH cluster of green space is found in the same area. This relation was found in some areas that not affected SUHI's in North Denpasar. It indicates a relation between the high cover area of green space that can affect the low SUHI intensity in the area. The same relationship is also found in mangrove areas in South Denpasar. However, the relationship between the LL cluster of the green space and the HH cluster of SUHI does not occur. It shows that the high-intensity SUHI cluster on the east side of South Denpasar is influenced by factors other than green space. The other study (Estoque et al., 2017; Weng et al., 2004) shows a significant relationship between vegetation and surface temperature. The study used statistical analysis and a spatial transect to discover the relationship between the two. On the other hand, this study compared the variable using the spatial pattern of data clusters. Therefore, that the relationship between variables can be identified if it has a significant cluster.

Whereas, the SUHI and moisture index have a relationship at the HH moisture cluster with an LL SUHI cluster. The area is located on the north and south sides of Denpasar. However, the HH cluster of SUHI does not show a significant cluster of surface moisture. The high surface moisture cluster is in a flooded area (rice fields and mangrove areas). The relationship between SUHI and built-up density is demonstrated by the low built-up density cluster with a low SUHI cluster. The relation between high built-up density and high-SUHI intensity only occurs in some downtown areas, but the area with a high SUHI intensity cluster does not show a significant cluster of built-up density. The built-up density map shows a similar pattern to the surface moisture cluster. The high built-up density is accompanied by low surface moisture in the downtown area. Based on the relationship between the variables, it can be known that the relationship between green space and surface urban heat islands occurs in the North and South Denpasar. The relationship is shown by the existence of the low SUHI intensity that accompanies by a high green space cover cluster. However, the relationship between the LL cluster of the green space and the HH cluster of SUHI does not occur. It indicates other factors can affect the SUHI phenomenon. The surface moisture index shows a relationship with the SUHI, especially at a high moisture index accompanied by a low SUHI intensity. However, the relationship between high built-up density and high SUHI intensity only occurs in some areas of the downtown area.

The high SUHI intensity is dominant in the eastern region of South Denpasar. In addition to the low cluster of green space, it can also be influenced by the concentration of anthropogenic activity in that area. Areas with high SUHI intensity are the Sanur's coastal area which is a tourist destination and tourism industry area. The rise in heat sources can be influenced by the increase in anthropogenic activity following the opening of the tourism industry and no restrictions on community activities post-pandemic. According to the United States Environmental Protection Agency's (2008) explanation of the causative factors of UHI, which states that anthropogenic activities can influence SUHI patterns, particularly in the winter. These variables can have an impact on the difference in the SUHI patterns produced by the two images taken at

different times.

4. CONCLUSION

The urban green space in Denpasar city covers a 28.22 km2 area, which consists of 14.12 km2 of public green space and 14.10 km2 of private green space. The yard green space (private green space) is the largest green space cover, while the road green line type is the smallest cover with 1.12 km2. Denpasar's largest green space cover is 14.19 km2 (50.27%), located in the South Denpasar sub-district. The green space available in Denpasar only covers 22.1% of the administrative area, so it requires 8.85 km2 of additional green space. The SUHI phenomenon does not occur on Denpasar's north and south sides, which are dominated by rice fields (in the north) and mangrove forest areas (in the south). The majority of Denpasar has been affected by the SUHI phenomenon. The highest SUHI class was 4-5°C, which is found in east region of South Denpasar. The relationship between green space and SUHI occurs in north region of North Denpasar. It is identified in some areas with low-SUHI intensity clusters and high green space cover, but the relationship between High-SUHI intensity does not find in whole study area. The effect of surface humidity at the SUHI occurs at the high moisture index area that shows a low SUHI intensity. However, the low surface moisture area doesn't show a significant SUHI cluster. Moreover, the built-up density index shows a similar pattern with surface moisture. The relationship occurring in downtown areas is shown by a high built-up density which is accompanied by a low moisture index. It indicates that high-SUHI intensity can be influenced by other factors such as anthropogenic activity and surface conditions.

Author Contributions: Wirayuda, I., Widayani,P., and Sekaranom, A. conceived and designed the research and wrote the paper; Widayani, P. and Sekaranom, A. provide the research and analysis tools; Wirayuda I. performed the research.

Competing Interests: The authors declare no conflict of interest.

REFERENCES

Akbari, H., Pomerantz, M., & Taha, H. (2001). Cool surfaces and shade trees to reduce energy use and improve air quality in urban areas. *Solar energy, 70*(3), 295-310. https://doi.org/10.1016/S0038-092X(00)00089-X

Anselin, L. (1994). Exploratory spatial data analysis and geographic information systems. *New Tools for Spatial Analysis, 17,* 45–54.

Asmiwyati, I. G. A. A. R., Sugianthara, A. A. G., & Wardi, I. N. W. (2020). Identifikasi suhu permukaan terhadap penutupan lahan dari Landsat 8: Studi Kasus Kota Denpasar. *Jurnal Arsitektur Lansekap, 6*(2), 240–246. https://doi.org/10.24843/JAL.2020.v06.i02.p11

As-syakur, A. R., Nuarsa, I. W., Arthana, I. W., Mahendra, M. S., Adnyana, I. W. S., Merit, I. N., ... & Lila, K. A. (2012). Remote Sensing Image-Based Analysis of The Urban Heat Island in Denpasar, Indonesia. 8th International Symposium on Lowland Technology, 997–1004.

Carlson, T. N., & Ripley, D. A. (1997). On the relation between NDVI, fractional vegetation cover, and leaf area index. *Remote Sensing of Environment, 62*(3), 241–252. https://doi.org/10.1016/S0034-4257(97)00104-1

Estoque, R. C., Murayama, Y., & Myint, S. W. (2017). Effects of landscape composition and pattern on land surface temperature: An urban heat island study in the megacities of Southeast Asia. *Science of the Total Environment, 577,* 349-359. https://doi.org/10.1016/j.scitotenv.2016.10.195

Fawzi, N. I. (2014). Pemetaan emisivitas permukaan menggunakan indeks vegetasi. *Majalah Ilmiah Globe, 16*(2), 133-139.

Gittleman, J. L., & Kot, M. (1990). Adaptation: statistics and a null model for estimating phylogenetic effects. *Systematic Zoology, 39*(3), 227-241. ehttps://doi.org/10.2307/2992183

Griffith, D. (2005). *Spatial Autocorrelation.* Syracuse University.

Grimm, N. B., Foster, D., Groffman, P., Grove, J. M., Hopkinson, C. S., Nadelhoffer, K. J., ... & Peters, D. P. (2008). The changing landscape: ecosystem responses to urbanization and pollution across climatic and societal gradients. *Frontiers in Ecology and the Environment, 6*(5), 264-272. https://doi.org/10.1890/070147

Johnson, J. M. F., Franzluebbers, A. J., Weyers, S. L., & Reicosky, D. C. (2007). Agricultural opportunities to mitigate greenhouse gas emissions. *Environmental Pollution, 150*(1), 107-124. https://doi.org/10.1016/j.envpol.2007.06.030

Karl, T. R., Diaz, H. F., & Kukla, G. (1988). Urbanization: Its detection and effect in the United States climate record. *Journal of Climate, 1*(11), 1099-1123.

Lee, J., & Wong, D. W. S. (2001). *Statistical analysis with ArcView GIS*. John Wiley & Sons.

Li, J., Song, C., Cao, L., Zhu, F., Meng, X., & Wu, J. (2011). Impacts of landscape structure on surface urban heat islands: A case study of Shanghai, China. *Remote Sensing of Environment, 115*(12), 3249-3263. https://doi.org/10.1016/j.rse.2011.07.008

Lillesand, T., Kiefer, R. W., & Chipman, J. (2015). *Remote sensing and image interpretation.* John Wiley & Sons.

Lo, C. P., & Quattrochi, D. A. (2003). Land-use and land-cover change, urban heat island phenomenon, and health implications: A remote sensing approach. *Photogrammetric Engineering and Remote Sensing, 69*(9), 1053- 1063. https://doi.org/10.14358/PERS.69.9.1053

Ma, Y., Kuang, Y., & Huang, N. (2010). Coupling urbanization analyses for studying urban thermal environment and its interplay with biophysical parameters based on TM/ETM+ imagery. *International Journal of Applied Earth Observation and Geoinformation, 12*(2), 110-118. https://doi.org/10.1016/j.jag.2009.12.002

Memon, R. A., Leung, D. Y., & Chunho, L. (2008). A review on the generation, determination and mitigation of Urban Heat Island. *Journal of Environmental Sciences, 20(*1), 120-128. https://doi.org/10.1016/S1001-0742(08)60019-4

Quattrochl, D. A., Luvall, J. C., Rickman, D. L., Estes Jr, M. G., Laymon, C. A., & Howell, B. F. (2000). A decision support information system for urban landscape management using thermal infrared data. *Photogrammetric Engineering & Remote Sensing, 66*(10), 1195-1207.

Rouse, J. W., Haas, R. H., Schell, J. A., & Deering, D. W. (1974). Monitoring vegetation systems in the Great Plains with ERTS. *IEEE Transactions on Geoscience Electronics, 11*(1), 3-76. https://doi.org/10.1109/TGE.1973.294284

Sass, R. L., & Cicerone, R. J. (2002). Photosynthate allocations in rice plants: Food production or atmospheric methane? *Proceedings of the National Academy of Sciences, 99*(19), 11993–11995. https://doi.org/10.1073/pnas.20248359

Setiawan, H., Mathieu, R., & Thompson-Fawcett, M. (2006). Assessing the applicability of the V-I-S model to map urban land use in the developing world: A case study of Yogyakarta, Indonesia. *Computers, Environment and Urban Systems, 30*(4), 503–522. https://doi.org/10.1016/j.compenvurbsys.2005.04.003

Stathopoulou, M., & Cartalis, C. (2007). Daytime urban heat islands from Landsat ETM+ and Corine land cover data: An application to major cities in Greece. *Solar Energy, 81*(3), 358–368. https://doi.org/10.1016/j.solener.2006.06.014

United States Environmental Protection Agency. (2008). Urban Heat Island basics. In

Reducing Urban Heat Islands: Compendium of Strategies; Chapter 1; Draft Report.
USGS. (2013). Using the USGS Landsat Level-1 Data Product.
Utomo, A. W., Suprayogi, A., & Sasmito, B. (2017). Analisis hubungan variasi land surface temperature dengan kelas tutupan lahan menggunakan data citra satelit landsat (Studi Kasus: Kabupaten Pati). *Jurnal Geodesi Undip, 6*(2), 71–80.
Voogt, J. A., & Oke, T. R. (2003). Thermal remote sensing of urban climates. *Remote Sensing of Environment, 86*(3), 370–384. https://doi.org/10.1016/S0034-4257(03)00079-8
Weng, Q., Lu, D., & Schubring, J. (2004). Estimation of land surface temperature-vegetation abundance relationship for urban heat island studies. *Remote Sensing of Environment, 89*(4), 467–483. https://doi.org/10.1016/j.rse.2003.11.005
Yamamoto, Y. (2006). Measures to Mitigate Urban Heat Islands. *NISTEP Science & Technology Foresight Center, 18,* 67–83.
Zha, Y., Gao, J., & Ni, S. (2003). Use of normalized difference built-up index in automatically mapping urban areas from TM imagery. *International Journal of Remote Sensing, 24*(3), 583–594. https://doi.org/10.1080/01431160304987